Pt-H complexes in Si: Complementary studies by vibrational and capacitance spectroscopies

M. G. Weinstein,* Michael Stavola,† Kathryn L. Stavola, and S. J. Uftring‡
Department of Physics, Lehigh University, Bethlehem, Pennsylvania 18015

J. Weber and J.-U. Sachse§
Technische Universität Dresden, D-01062 Dresden, Germany

H. Lemke
TU Berlin, Institut für Werkstoffe der Elektrotechnik, Jebensstraße 1, D-10623 Berlin, Germany
(Received 28 June 2001; published 19 December 2001)

The PtH and PtH_2 complexes in Si have been studied by vibrational and transient-capacitance spectroscopies in the same, or similarly prepared, samples. Further, the levels of the PtH and PtH_2 defects have been determined from their vibrational spectra and the vibrational lines have been associated with specific charge states of the defects. These results confirm that both vibrational spectroscopy and transient-capacitance methods probe the same defect complexes. These results also provide strong support for the previous assignments of deep level transient spectroscopy peaks to PtH and PtH_2 complexes that were made on the basis of the depth dependence of defect-concentration profiles that were measured for etched Si samples. The intensities of the vibrational lines of the PtH and PtH_2 complexes have also been calibrated so that the concentrations of these defects can be estimated from their vibrational spectra.

DOI: 10.1103/PhysRevB.65.035206 PACS number(s): 61.72.Ji, 63.20.Pw, 71.55.−i

I. INTRODUCTION

In pioneering studies of the hydrogen passivation of deep-level defects in semiconductors, it was discovered that the exposure of a Si sample to a hydrogen-containing plasma can eliminate many of the levels associated with the transition-metal impurities.[1–4] Until recently, little was known about the microscopic properties of the hydrogenated defects or about how hydrogen affected the electronic states. A variety of recent studies provide new insights, but also show that the hydrogenated transition-metal impurities are more complicated than the early studies suggested.[5–29]

New results have come from several approaches. A few groups used wet-chemical etching at room temperature to introduce hydrogen into thin surface layers of Si samples that also contained a transition-metal impurity.[5–8] In these studies, different electrically active, transition-metal H complexes were discovered and characterized by deep level transient spectroscopy (DLTS). Independently, it was found that H could be introduced throughout bulk Si samples by annealing in H_2 gas at elevated temperature (1250 °C) and that Pt impurities could be hydrogenated by this method.[9–11] PtH_2 and PtH centers were discovered and studied by electron paramagnetic resonance (EPR) and infrared (IR) absorption spectroscopies. In these studies, a structure for the PtH_2 defect was proposed and the PtH_2 and PtH complexes were found to be electrically active. In subsequent work, many transition-metal H complexes were produced by etching and studied by DLTS,[12–17] and a few additional transition-metal H complexes were studied by EPR (Ref. 18) and IR (Ref. 19) spectroscopies. Furthermore, theoretical calculations have been performed for several transition-metal H complexes to determine the structures of the complexes and also to calculate the H-stretching frequencies and the electronic level positions.[20–22]

There are only a few transition-metal H complexes for which both structure-sensitive data and DLTS results have been reported. And for these complexes, it is difficult to be certain that the different spectroscopic techniques, applied to samples fabricated by different methods, do indeed probe the same defect complexes. In recent DLTS studies, an important advance toward assigning the DLTS peaks to specific transition-metal H complexes has been made.[23–29] It was proposed that the number of hydrogen atoms in the transition-metal H complexes can be determined from an analysis of the depth dependence of the defect-concentration profiles measured for etched samples by DLTS.[23] A model for the introduction of H by etching predicts that the H concentration will decay exponentially with depth d into the sample. The concentration of H-containing complexes, $[A\mathrm{H}_n]$, was also predicted to decay exponentially with depth, and with a decay length that is inversely proportional to the number of H atoms n in the complex, or

$$[A\mathrm{H}_n] \propto \exp[-d(n/L)]. \tag{1}$$

The depth dependence of the concentration profiles has been measured for many of the DLTS features reported for the transition-metal H complexes in Si and the numbers of H atoms in the complexes have been deduced from the slopes of the $\ln[A\mathrm{H}_n]$ vs depth profiles.[24–29]

In this paper, we report the results of experiments on the PtH and PtH_2 complexes in Si that correlate complementary IR absorption and DLTS measurements. The Pt-H complexes have been studied by DLTS,[15,16,28] EPR,[9,10] and vibrational spectroscopy[9,11] and therefore provide an excellent model system to test the assignments that are based upon an analysis of the DLTS concentration profiles and also to confirm that the same transition-metal H complexes are produced by the different hydrogenation methods. The frequencies of the

 ©2001 The American Physical Society

TABLE I. Frequencies of the H-stretching lines assigned to the different charge states of PtH and PtH_2 complexes in Si (in units cm^{-1}). For PtH_2, the frequencies of the antisymmetric- and symmetric-stretching modes (AS and SS, respectively) are given (from Ref. 11).

Complex	Charge state	Frequency (cm^{-1})	
PtH	$m-1$	1897.2	
	m	1880.7	
		AS	SS
PtH_2	$n-2$	1889.6	1898.0
	$n-1$	1888.2	1901.6
	n	1873.1	1891.9

H-stretching vibrational lines assigned to the different charge states of the PtH and PtH_2 complexes observed for Si samples hydrogenated at 1250 °C throughout the bulk are given in Table I. The DLTS levels and their assignments for PtH, PtH_2, and PtH_3 complexes studied in Si samples that were hydrogenated by wet-chemical etching at room temperature are given in Table II.

To determine whether the same PtH and PtH_2 complexes are indeed being studied by the different measurement techniques applied to samples fabricated by different hydrogen introduction methods, several experiments have been performed. Vibrational spectroscopy and DLTS were used to study samples prepared from the same Si boule into which Pt and H had been introduced during crystal growth.[16] Vibrational spectroscopy experiments were also performed on samples where hydrogen had been introduced by wet-chemical etching to confirm that the previously identified PtH and PtH_2 vibrational lines[11] are also produced by this hydrogenation method. Further, the positions of the electronic levels associated with the PtH and PtH_2 complexes seen by vibrational spectroscopy are estimated. The level positions determined from the vibrational spectra are then compared with those determined previously by DLTS (Refs. 16 and 28) to complete the association of the vibrational lines with specific charge states of the PtH and PtH_2 complexes. Finally, complementary DLTS and IR absorption data are used to calibrate the intensities of the H-stretching lines so that the concentrations of PtH and PtH_2 complexes produced in the different samples can be determined.

II. EXPERIMENT

Silicon samples that contained Pt and H were prepared by several different methods for our experiments.

TABLE II. List of energy levels, activation enthalpies, and assignments for the DLTS peaks observed for Si that contained Pt and H impurities (from Refs. 16 and 28).

Level	H_A (eV)	Assignment
$E(90)$	$E_C-0.16$	$PtH_2(=/-)$
$E(250)$	$E_C-0.50$	PtH $(-/0)$
$H(210)$	$E_V+0.40$	PtH_2 $(-/0)$
$H(150)$	$E_V+0.30$	PtH_3

(i) For a few samples, Pt was added to the Si melt during crystal growth by the floating zone method (with an Ar ambient). These samples were n-type with $[P]=4.5\times10^{14}\,cm^{-3}$. In previous experiments,[16] these samples were found to contain hydrogen that had been introduced unintentionally throughout the bulk of the material. Presumably the source of hydrogen was either a small, unintentional concentration of H in the Ar growth ambient or water-vapor contamination from the growth chamber.

(ii) Pt was introduced into several bulk Si samples by high-temperature diffusion. Starting materials were n- or p-type floating zone silicon ($[P]=3\times10^{16}\,cm^{-3}$ or $[B]=2\times10^{15}\,cm^{-3}$, respectively) or n-type Czochralski-grown silicon ($[As]=2\times10^{16}\,cm^{-3}$). First, Pt was diffused into these samples by annealing for 18 h in a sealed quartz ampoule that contained Pt powder and a He ambient. Following the diffusion heat treatment, the samples were etched in a CP4 solution (1:2:1 mixture of $HF:HNO_3:CH_3COOH$ acids) to remove any remaining Pt from the sample surfaces. Hydrogen was then introduced throughout the bulk of these Si:Pt samples by an annealing treatment at 1250 °C for 30 min in a sealed quartz ampoule filled with 0.7 atm of H_2 gas. The high-temperature anneal was terminated by a rapid quench to room temperature in water.

(iii) For the multiple-internal-reflection measurements to be discussed in Sec. III, samples were prepared by diffusing Pt into n- or p-type silicon samples at 1250 °C for 18 h. The sample surfaces were then polished and the end surfaces were beveled to a 45° angle. Typical sample dimensions were $14\times18\times2\,mm^3$. The samples were subsequently annealed at 700 °C in flowing N_2 to eliminate any small concentration of PtH or PtH_2 complexes that might have been unintentionally formed by H introduced into the sample during the Pt diffusion treatment. Vibrational spectra measured following this anneal and before wet-chemical etching showed none of the vibrational lines previously assigned to PtH or PtH_2 centers. Finally, hydrogen was introduced into thin surface layers by either a white etch (10:2 mixture of $HNO_3:HF$ acids) or a CP4 etch.

IR absorption measurements were made with a Bomem DA3.16 Fourier transform spectrometer equipped with a KBr beamsplitter and InSb and HgCdTe detectors. Spectra were recorded near liquid-helium temperature. A resolution of 0.35 cm^{-1} was used in the H-stretching range (>1800 cm^{-1}). A 5-μm (2000-cm^{-1}) low-pass filter was inserted in front of the sample for our measurements of the H-stretching spectra to reduce the photoionization of defects caused by the spectrometer light. Slowly varying residual baselines that had not been completely eliminated by the reference samples were subtracted from our data to produce the absorbance spectra reported here. Spectra shown in the figures thoughout this paper are shifted from their zero baselines for the purposes of presentation. Shallow-dopant concentration profiles were determined from capacitance-voltage (CV) measurements made at 1 MHz. Transient-capacitance spectroscopy was performed with a computer-controlled DLTS system. During DLTS concentration-depth profiling,[30] the sample was held at constant reverse bias and the filling pulse height was varied. EPR measurements were performed with a 14-

GHz spectrometer. Electron irradiations were performed with a 2.5-MeV Van de Graaff accelerator to vary the Fermi-level position in some *n*-type samples. All of the samples were irradiated at room temperature and were mounted on a water-cooled plate to prevent sample heating.

III. COMPLEMENTARY STUDIES BY VIBRATIONAL AND CAPACITANCE SPECTROSCOPIES

The different sample characteristics required for DLTS and IR absorption measurements of the transition-metal H complexes usually make measurements by both techniques on the same samples impractical. In this section a few cases are described where IR absorption and DLTS measurements were made on the same, or similarly prepared, Si samples that contain Pt and H.

A. Vibrational spectroscopy and DLTS for Si:Pt samples grown by the floating zone method

Typical samples used in DLTS studies of the transition-metal H complexes[12–17,24–29] contain an insufficient number of defects ($<10^{14}\,\mathrm{cm}^{-3}$ in 3-μm-thick layers) to be studied by vibrational spectroscopy. Alternatively, the samples produced for IR absorption experiments[9,11,19] where the transition metal and H are introduced by high-temperature annealing and quenching are usually treated too roughly for reliable DLTS measurements. Si samples for which it has been possible to perform both DLTS and IR absorption experiments were grown by the floating zone method. These samples were intentionally doped with Pt and unintentionally doped with H during growth and contained Pt and H throughout the bulk.[16] DLTS spectra obtained for these samples [Fig. 1(a)] show the DLTS peaks assigned previously (Table II) to Pt($-$/0), PtH($-$/0), and $\mathrm{PtH_2}(=/-)$. Figure 2 shows the vibrational spectrum of a sample with a thickness of 1.5 cm that was prepared from a nearby piece of the same crystal. The vibrational lines seen in Fig. 2 have the same frequencies as lines assigned previously to the PtH and $\mathrm{PtH_2}$ complexes (Table I).

The spectra shown in Figs. 1(a) and 2 should be compared with caution. The DLTS peaks arise primarily from the near surface region where H had been introduced by the wet etch that preceded the deposition of the Schottky barrier used to perform the capacitance measurements. The concentration profiles measured for the $\mathrm{PtH_2}$ [$E(90)$] and PtH [$E(250)$] peaks by DLTS [Fig. 1(b)] show that these defects extend into the bulk of the sample where their concentrations were found to be $2\times10^{12}\,\mathrm{cm}^{-3}$ and $1\times10^{13}\,\mathrm{cm}^{-3}$, respectively. It is primarily this smaller concentration of centers, with greater total number because they are distributed throughout the bulk of the sample, to which the IR absorption measurements are sensitive.

These complementary DLTS and IR absorption data confirm that the PtH and $\mathrm{PtH_2}$ centers studied by vibrational spectroscopy and by DLTS are present in the same samples. From these data, the IR absorption intensities can be calibrated (see Sec. V) so the concentrations of the PtH and $\mathrm{PtH_2}$ complexes can be determined from their IR spectra.

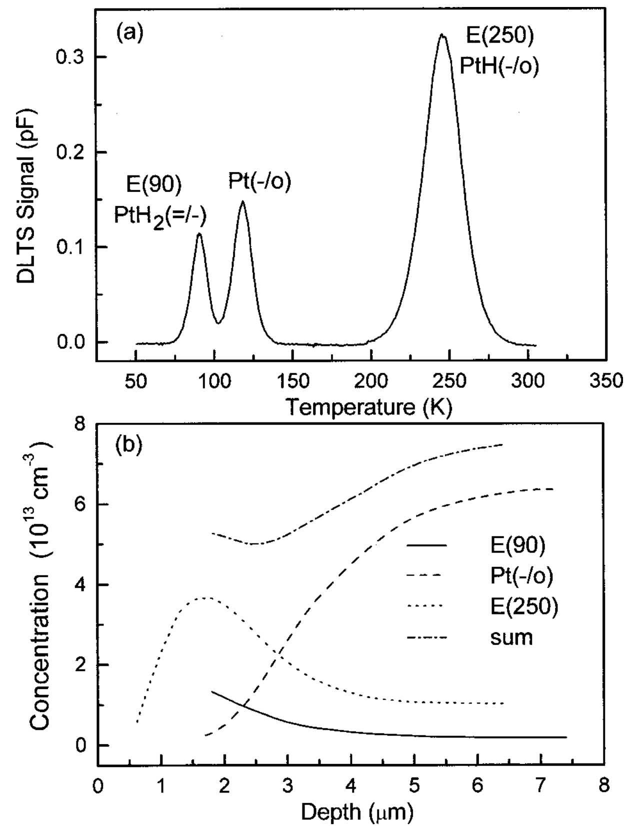

FIG. 1. (a) DLTS spectrum and (b) defect-concentration profiles for a sample cut from a Si crystal that was intentionally doped with Pt and unintentionally contaminated with H during growth by the floating zone method. The sample was etched prior to the fabrication of a Schottky barrier contact, introducing additional H into the near surface region.

B. Vibrational spectroscopy for Si:Pt samples hydrogenated by wet-chemical etching

The thin surface layers of Pt- and H-containing complexes which are formed when samples are hydrogenated by wet-chemical etching are unsuitable for vibrational absorption

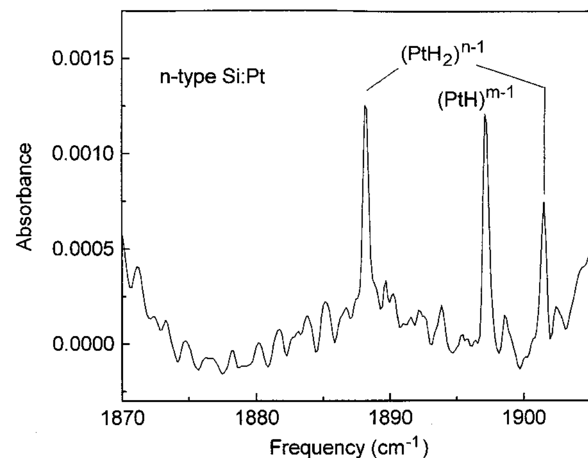

FIG. 2. IR absorption spectrum for a nearby piece of the same crystal used for the DLTS data presented in Fig. 1. The optical path length was 1.5 cm.

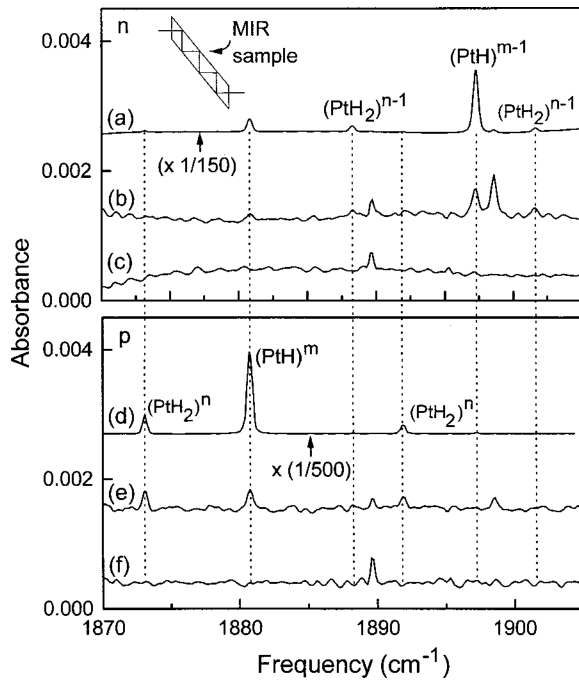

FIG. 3. IR absorption spectra for *n*-type (upper) and *p*-type (lower) Si:Pt samples. The inset in the upper panel shows the geometry for a MIR measurement. Spectra (a) and (d) show, for reference, the H-stretching lines of the PtH and PtH_2 complexes observed in bulk-hydrogenated Si:Pt samples. Spectra (b) and (e) were measured for *n*- and *p*-type Si:Pt MIR samples, respectively, that had been hydrogenated by wet-chemical etching and annealed at 200 °C. Spectra (c) and (f) were measured for the same MIR samples but after they had been lapped and repolished.

measurements made with the spectrometer light at normal incidence due to the sensitivity limitations of the technique. However, multiple-internal-reflection (MIR) methods,[31] in which two opposite ends of the sample are beveled so that the light is multiply reflected from the internal sample surfaces tens of times, can greatly increase the sensitivity of IR absorption measurements to thin surface layers (see the inset in Fig. 3). Si:Pt MIR samples were fabricated to investigate the introduction of H by wet-chemical etching by vibrational spectroscopy.

Figure 3 shows spectra for *n*- and *p*-type Si:Pt MIR samples. Spectra (a) and (d) in Fig. 3 show, for reference, the H-stretching lines previously assigned to the PtH and PtH_2 complexes for *n*- and *p*-type Si:Pt samples with [Pt]>[P] and [Pt]>[B], respectively (Ref. 11 and Table I). These spectra were measured with light at normal incidence for samples that were hydrogenated throughout the bulk by a high-temperature anneal in H_2 gas. Spectra (b) and (e) in Fig. 3 were measured for the *n*- and *p*-type Si:Pt MIR samples following a wet-chemical etching treatment performed at room temperature and a subsequent 200 °C anneal that was found to increase the concentrations of PtH and PtH_2 complexes.[32] DLTS profiles of similarly etched and annealed samples showed that H typically had diffused into the sample to a depth of approximately 3 μm.[16,28] In spectrum (b), the PtH and PtH_2 vibrational lines seen previously[11] in *n*-type Si that contained Pt and H are visible. In spectrum (e), the lines seen previously[11] in *p*-type Si that contained Pt and H are visible. Although the PtH and PtH_2 lines shown for the MIR samples in Fig. 3 are weak, their dependence on material type, with the more negative charge states of the complexes appearing only for the *n*-type starting material [spectrum (b)] and the more positive charge states only for the *p*-type starting material [spectrum (e)], strongly supports their identification.

Spectra (c) and (f) in Fig. 3 were measured for the same wet-etched samples as for (b) and (e), respectively, but after the samples had been lapped and repolished. The vibrational lines introduced by the etching treatment were no longer present after thin surface layers had been removed, confirming that the PtH and PtH_2 lines in the MIR samples did indeed come from H that had been introduced near the sample surfaces by the etch. [The thickness of the *p*-type sample, spectra (e) and (f), was carefully measured with a micrometer before and after each surface was lapped and polished to show that ≈50 μm had been removed from each surface.]

In addition to the vibrational lines assigned previously to the PtH and PtH_2 complexes, a line at 1898.6 cm^{-1}, seen previously in Si that contained Pt and H throughout the bulk[11] but not assigned to either the PtH or PtH_2 complex,[33] was also observed. This line is present in both *n*- and *p*-type Si:Pt MIR samples, indicating that there is no level in the upper half of the Si band gap associated with this line. Thus the data show that the 1898.6-cm^{-1} line is not related to the DLTS peaks assigned to the PtH and PtH_2 complexes seen in *n*-or *p*-type samples. In the spectra shown in Fig. 3, an additional line near 1890 cm^{-1} is also present. This line is coincident with a strong line due to H_2O vapor present in the spectrometer and is not related to any Pt-H complexes.

The increased sensitivity provided by the MIR measurements and the sharpness of the vibrational lines have led to the remarkable capability to characterize by vibrational spectroscopy the small numbers of PtH and PtH_2 centers present in the thin, hydrogenated surface layers produced by wet-chemical etching. The concentrations of centers observed will be estimated in Sec. V. These experiments, in which the previously assigned vibrational modes of PtH and PtH_2 complexes were observed in samples hydrogenated by wet etching, provide additional evidence that the Pt- and H-related defects studied previously by EPR and vibrational spectroscopies and by DLTS are due to the same defect complexes.

IV. LEVEL POSITIONS FROM THE FERMI-LEVEL DEPENDENCE OF THE VIBRATIONAL SPECTRA

In this section, upper and lower limits are determined for the electronic-level positions of the PtH and PtH_2 complexes studied by vibrational spectroscopy so that the vibrational lines associated with different charge states (Table I) can be related to the levels observed in DLTS experiments (Table II). To determine level positions by vibrational spectroscopy, we take advantage of the shift (roughly 20 cm^{-1}) in the vibrational frequency of the H-stretching lines that occurs for the different charge states of the same transition-metal H

complex.[11] From the relative intensities of the vibrational lines, the relative populations of the different charge states of a defect can be monitored as the Fermi level in the sample is varied. By preparing samples with Fermi levels pinned at several known energies in the Si band gap, the position of each PtH or PtH_2 defect level relative to these Fermi-level "markers" can be determined, thus determining upper and lower limits for the energies of the defect levels.

A. Compensation by transition-metal doping

Both Pt and Au impurities in Si have acceptor and donor levels whose energies are well known.[34,35] (Pt has acceptor and donor levels at $E_C-0.23$ eV and $E_V+0.32$ eV, respectively. Au has acceptor and donor levels at $E_C-0.55$ eV and $E_V+0.35$ eV, respectively.) The indiffusion temperatures for these transition-metal impurities were selected to produce Si samples with metal concentrations that were either smaller or greater than the shallow dopant concentration and therefore with different Fermi-level positions. It is important to note that the precise concentrations of the Pt and Au impurities do not need to be known, only whether the concentration is greater or less than the shallow dopant concentration. Thus estimates of the concentrations of Pt and Au in our samples made from their previously measured solubilities[34,35] were sufficiently accurate for our purposes. The introduction of H into the samples did not appreciably affect the Fermi-level position determined by the shallow dopants and transition-metal impurities. Donor-H complexes are not formed by the introduction of H from H_2 gas at high temperature[36] and the H-stretching line of the B-H complex was not seen in our *p*-type samples. Further, it will be shown that only a fraction of the transition-metal concentration is hydrogenated in our samples (Sec. V), making the isolated metal impurity the dominant compensating defect.

To produce samples with a low Pt concentration (relative to $[P]=3\times10^{16}\,cm^{-3}$), a diffusion temperature of 950 °C was used. From previous solubility data,[34,35] the Pt concentration was estimated to be $[Pt]\approx4\times10^{15}\,cm^{-3}$. To produce samples with a high Pt concentration, a diffusion temperature of 1250 °C was used. In this case, the Pt concentration was estimated to be $[Pt]\approx1\times10^{17}\,cm^{-3}$. EPR was used to confirm the position of the Fermi level for a few of the Pt-diffused samples into which H had also been introduced. For samples prepared with a P concentration of $[P]=3\times10^{16}\,cm^{-3}$ and a Pt indiffusion temperature of $T=950\,°C$, the P^0 EPR spectrum remained visible (P is paramagnetic when neutral) showing that the Fermi level remained locked to the P(0/+) level. Alternatively, for samples with a Pt indiffusion temperature of 1250 °C, EPR measurements showed that the P was in its nonparamagnetic charge state P^+, confirming that the Fermi level had been lowered, presumably to the now dominant acceptor level of Pt at $E_C-0.23$ eV. In addition to the samples containing P and Pt, a few other samples were prepared. An *n*-type sample with $P=3\times10^{16}\,cm^{-3}$ was indiffused with Pt at 950 °C and, in a subsequent diffusion treatment after excess Pt had been removed from the samples surfaces, with Au at 1250 °C. Previous solubility data[34,35] were used to select these diffusion temperatures in order to produce Pt and Au concentrations of $\approx4\times10^{15}\,cm^{-3}$ and $\approx1\times10^{17}\,cm^{-3}$, respectively, and consequently a Fermi level near the Au acceptor level at $E_C-0.55$ eV. A *p*-type sample with $[B]=2\times10^{15}\,cm^{-3}$ was indiffused with Pt at 1250 °C to produce an estimated Pt concentration of $[Pt]\approx1\times10^{17}\,cm^{-3}$, and consequently a Fermi level at low temperature near the Pt donor level at $E_V+0.32$ eV.

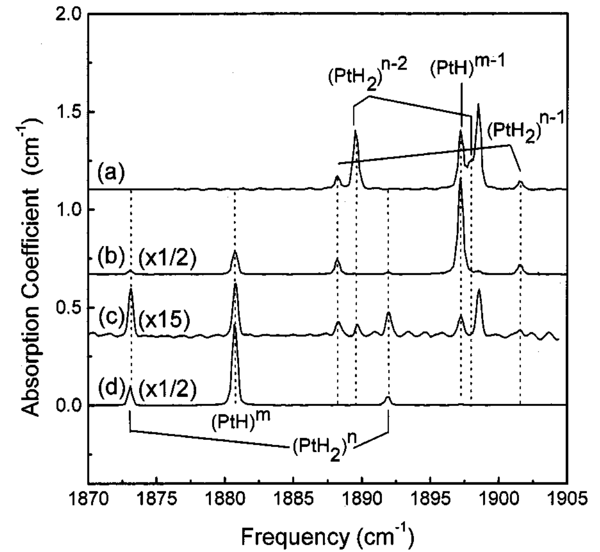

FIG. 4. H-stretching spectra of PtH and PtH_2 complexes in Si for successively lower positions of the Fermi level. Fermi-level position and sample preparation details (starting material type and metal diffusion temperature T_D) are as follows: (a) $E_C-0.045$ eV (*n* type, Pt with $T_D=950\,°C$); (b) $E_C-0.23$ eV (*n* type, Pt with $T_D=1250\,°C$); (c) $E_C-0.55$ eV (*n* type, Pt with $T_D=950\,°C$ and Au with $T_D=1250\,°C$); (d) $E_V+0.32$ eV (*p* type, Pt with $T_D=1250\,°C$).

Figure 4 shows vibrational spectra for samples with their Fermi-level positions located successively lower in the Si band gap. The superscripts give the charge states of the PtH and PtH_2 complexes. In spectra (a) through (d), the more positive charge states of the PtH and PtH_2 complexes become populated as the Fermi level is located successively lower in the band gap. For example, spectrum (a) in Fig. 4 is for an *n*-type sample with a low Pt concentration and thus a Fermi level near the P level at $E_C-0.045$ eV. This spectrum shows the vibrational lines associated with the $(PtH)^{m-1}$ and $(PtH_2)^{n-2}$ charge states. Spectrum (d) is for a *p*-type sample with a high Pt concentration. In this case, with the Fermi level near the Pt donor level at $E_V+0.32$ eV, the only vibrational lines seen are those for the most positive charge states of both complexes, $(PtH)^m$ and $(PtH_2)^n$.

B. Compensation by electron irradiation

Electron irradiation was also used to controllably vary the position of the Fermi level in a few samples to further refine the determination of the electronic level positions of the transition-metal H complexes. Two common irradiation-produced defect levels are of particular interest here.[37] The electron irradiation of Czochralski-grown (oxygen-rich)

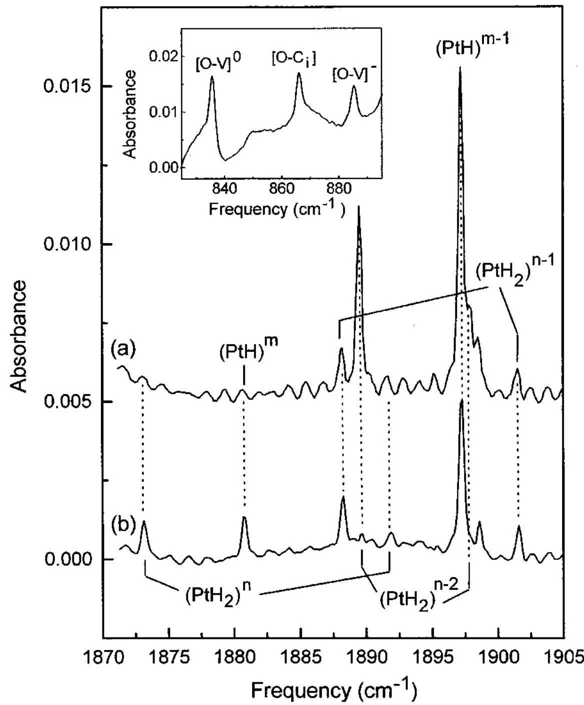

FIG. 5. H-stretching spectra for the PtH and PtH_2 complexes in Czochralski-grown *n*-type Si. The spectra were measured (a) before and (b) after a 2.5-MeV electron irradiation with a fluence of $8 \times 10^{16}\,cm^{-2}$. The inset shows the vibrational lines of the neutral and negative charge states of the O-V complexes (measured with 1-cm^{-1} resolution) that were observed in the same Si sample following the 2.5-MeV electron irradiation. (A vibrational line due to a complex of oxygen with interstitial carbon, Ref. 39, is also produced by the irradiation.)

n-type Si produces oxygen-vacancy complexes (or *A* centers) with an acceptor level at $E_C - 0.17\,eV$. The electron irradiation of floating zone (low oxygen content), *n*-type Si produces, as the dominant defect, donor-vacancy complexes (or *E* centers). The P-V complex has an acceptor level at $E_C - 0.43\,eV$. *N*-type samples containing Pt and H were electron irradiated to move the Fermi level from near the conduction-band edge to each of these levels. Infrared absorption and EPR spectroscopies were used to monitor the charge states of the irradiation-produced defects as a cross check of the Fermi-level position.[38]

Figure 5 shows the H-stretching spectra of the PtH and PtH_2 complexes in a Czochralski-grown Si sample (a) before and (b) after an electron irradiation with a fluence of $8 \times 10^{16}\,e^-/cm^2$. This sample was initially *n* type with $[As] = 2 \times 10^{16}\,cm^{-3}$, had an estimated Pt concentration of $\approx 1 \times 10^{16}\,cm^{-3}$ (produced by a diffusion treatment of 1000 °C), and had been hydrogenated throughout the bulk of the sample by a high-temperature anneal in hydrogen gas. Vibrational lines at 884 and 835 cm^{-1} that were previously assigned[39] to the negative and neutral charge states of the *A* center, respectively, were seen with roughly equal intensities in the same sample (inset in Fig. 5). This result indicates that the Fermi level had been lowered by the irradiation to near the acceptor level of the *A* center at $E_C - 0.17\,eV$. (Successive irradiations, each with a fluence of $2 \times 10^{16}\,e^-/cm^2$, were found to produce only the negative charge state of the *A* center for the lowest dose and then to produce an increasing fraction of the neutral state as the irradiation dose was increased.)

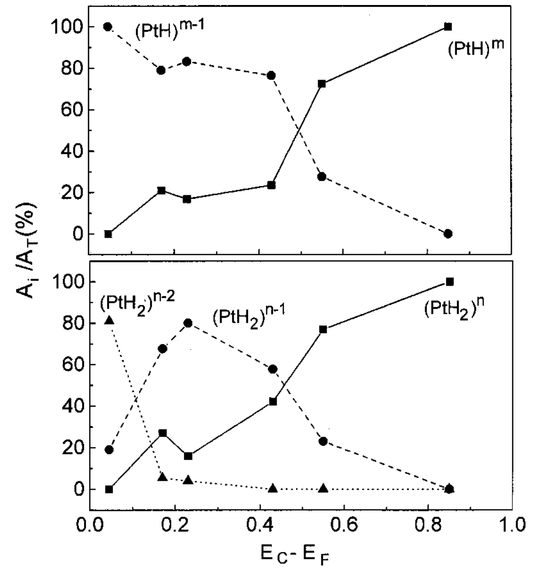

FIG. 6. Fraction of (a) PtH and (b) PtH_2 complexes in each charge state for different positions of the Fermi level.

A similar electron-irradiation experiment was performed for a Si:Pt+H sample fabricated from floating zone Si ($[P] = 3 \times 10^{16}\,cm^{-3}$). In this case, EPR was used to monitor the position of the Fermi level. Following electron irradiation with a fluence of $1 \times 10^{17}\,e^-/cm^2$, the EPR signal assigned to the *E* center (paramagnetic when neutral) was observed, showing that the Fermi level had been lowered to the acceptor level of the *E* center at $E_C - 0.43\,eV$. IR absorption spectra were measured before and after the electron irradiation to determine the relative populations of the different charge states of the PtH and PtH_2 defects in each case.

C. Correlation of the vibrational lines with the charge states and levels studied by DLTS

Figures 6(a) and (b) are a summary of our results and show the fractions of the PtH and PtH_2 defects in each of their possible charge states for different positions of the Fermi level. To determine the fraction of each defect in a specific charge state, the peak absorbance was measured for the H-stretching lines of the PtH and PtH_2 complexes for each Fermi-level position.[40] The peak absorbance A_i for each specific charge state was then divided by the sum of the absorbances A_T for all the charge states of that defect for each Fermi-level position. The fraction in each charge state determined in this way does not depend on the specific concentrations of PtH and PtH_2 complexes in the different samples and allows the data for different Fermi level positions to be compared.

Figure 6(a) shows that the $m-1$ charge state of PtH remains dominant while the position of the Fermi level is lowered from near the conduction-band edge E_C to the energy of the *E* center's acceptor level at $E_C - 0.43\,eV$. The *m* charge

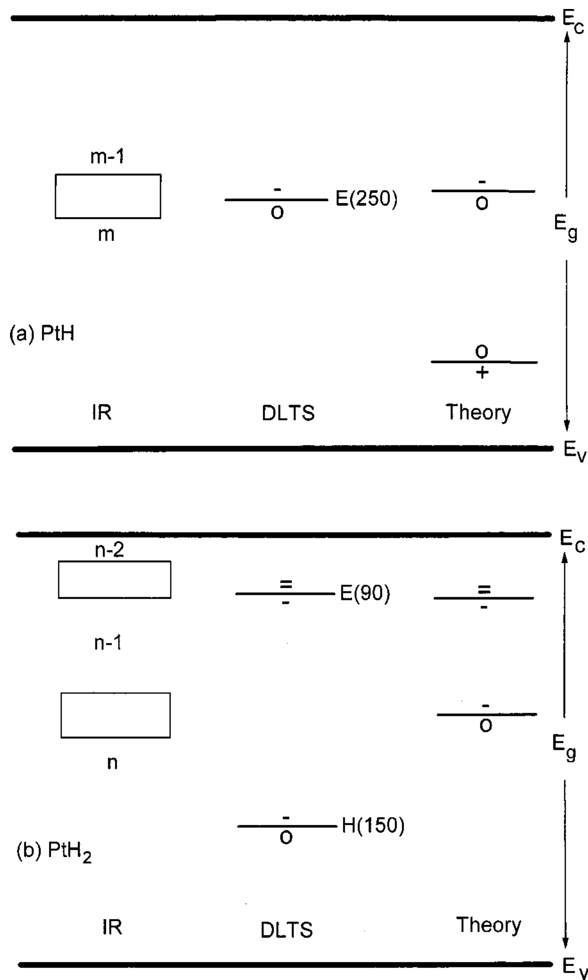

FIG. 7. Comparison of the energies of the electronic levels of (a) the PtH complex in Si and (b) the PtH_2 complex in Si that were determined by vibrational spectroscopy, DLTS (Ref. 28), and theory (Ref. 22).

state becomes dominant when the Fermi level is further lowered to the energy of the Au-acceptor level at $E_C - 0.55$ eV. These data indicate that the $m-1/m$ level of PtH lies between $E_C - 0.43$ eV and $E_C - 0.55$ eV as is shown in Fig. 7(a). Similarly, the changes that occur in the relative populations of the $n-2$, $n-1$, and n charge states of PtH_2 [Fig. 6(b)] as the Fermi level is lowered indicate that the $n-2/n-1$ level lies between the P donor level at $E_C - 0.045$ eV and the *A* center's acceptor level at $E_C - 0.17$ eV. These data also suggest that the $n-1/n$ level of PtH_2 lies between the acceptor levels of the *E* center and Au. These ranges for the levels of the PtH_2 complex are shown in Fig. 7(b).

Along with the limits for the level positions of the PtH and PtH_2 complexes determined above, Figs. 7(a) and (b) show the level positions for these defects that were determined previously by DLTS[16,28] (Table II) and also the level positions determined by theory.[22] A comparison of the level positions determined by vibrational spectroscopy with the DLTS results provides support for the assignment of the DLTS peaks to the same PtH and PtH_2 complexes that were identified by vibrational spectroscopy.[11] These results also allow the vibrational lines to be assigned to specific charge states.

Figure 7(a) shows that the energy of the $E(250)$ DLTS peak, previously assigned to the $(-/0)$ level of a PtH complex, and the range of energies for the $(m-1/m)$ level of PtH, determined by vibrational spectroscopy, are in excellent agreement. The vibrational lines at 1897.2 and 1880.7 cm^{-1} are therefore assigned to the $(-)$ and (0) charge states, respectively, of the PtH complex. (This assignment makes $m = 0$ in the charge state labels in Table I and the figures in this paper.)

Figure 7(b) shows the energies of the $E(90)$ and $H(150)$ DLTS peaks previously assigned to the $(=/-)$ and $(-/0)$ levels, respectively, of a PtH_2 complex. The range of energies for the $(n-2/n-1)$ level of PtH_2 determined by vibrational spectroscopy is in good agreement with the energy of the $(=/-)$ level found by DLTS. Therefore the vibrational lines at 1889.6 and 1898.0 cm^{-1} are assigned to the $(=)$ charge state and the lines at 1888.2 and 1901.6 cm^{-1} are assigned to the $(-)$ charge state of PtH_2. (This assignment makes $n=0$ in the charge state labels in Table I and the figures in this paper.)

The position of the $(n-1/n)$ level of PtH_2 found here is $\sim$0.25 eV higher in the Si band gap than the $(-/0)$ level for the PtH_2 complex found by DLTS [Fig. 7(b)]. A possible reason for this discrepancy is that light from the spectrometer can photoionize defects in the sample and change the populations of the different charge states from the equilibrium values that would be observed in darkness. While the spectrometer light was filtered to eliminate frequencies greater than the spectral range of interest, the incident light still had sufficient energy to ionize deep defects because the excitation of the H-stretching modes of the PtH and PtH_2 complexes requires roughly 0.25 eV. In previous studies,[11] we have found that the effect of the spectrometer light is to make the deeper charge states of the transition-metal H complexes appear in the vibrational spectra even though these charge states would not be populated in darkness. Indeed, we have used the photoinduced population of nonequilibrium charge states in our previous work to *identify* the different charge states of the PtH and PtH_2 defects.[11] The effect of the spectrometer light is to make the levels appear higher in the band gap than they actually are. We therefore associate the $(n-1/n)$ level observed by vibrational spectroscopy with the $(-/0)$ level of PtH_2 at $E_V + 0.4$ eV determined by DLTS. The vibrational lines at 1873.1 and 1891.9 cm^{-1} are assigned to the neutral charge state of the PtH_2 complex.

Figure 7 also shows the level positions of the PtH and PtH_2 complexes calculated by theory.[22] Previous studies have found the differences between the level positions calculated for the transition-metal H complexes and those determined experimentally to be $\approx$0.2 eV. The results in Fig. 7 show similar differences. [Neither DLTS nor vibrational studies find any evidence for the existence of the deep donor level of the PtH complex predicted by theory and shown in Fig. 7(a). It is possible that this level is too shallow to be detected or that it lies in the Si valence band.] We note that while the levels determined by vibrational spectroscopy are in better agreement with theory than the DLTS levels, especially for the acceptor level of the PtH_2 complex, the uncertainties in the level positions determined by vibrational spectroscopy or

theory are sufficiently great for the DLTS level positions to be considered the most reliable.

In a previous study of the different charge states of PtH_2 by EPR and vibrational spectroscopy, it was suggested that this defect is a double acceptor and that the =, −, and 0 charge states were being observed.[11] The correlation of the various charge states seen by vibrational spectroscopy with the DLTS levels and theory for the same PtH_2 defect are in agreement with this previous conclusion.

V. CONCENTRATIONS OF PtH AND PtH_2 COMPLEXES

The DLTS and IR absorption data shown in Figs. 1 and 2 were obtained for samples cut from nearby positions in the same Si:Pt boule and permit the intensities of the H-stretching lines of the PtH and PtH_2 complexes to be calibrated. The following equation[39,41] defines an effective oscillating charge q that relates the integrated absorption coefficient to the concentration N of absorbing centers:

$$\int \alpha d\bar{\nu} = \frac{\pi q^2 N}{nmc^2}. \qquad (2)$$

This equation has been written in cgs units to be consistent with the absorption coefficient α, conventionally determined in units cm^{-1}, and the frequency $\bar{\nu}=2\pi\omega/c$, given in wavenumber units. Here, m is the mass of the vibrating impurity, n is the refractive index of the host crystal, and c is the speed of light. (The baseline-corrected absorbance A, given in Fig. 2, is related to the absorption coefficient α by the relationship $A=\alpha x \log_{10} e$, where x is the optical path length of the absorbing sample.) From the data shown in Figs. 1(b) and 2, the effective charge associated with the 1897.2-cm^{-1} line of $(PtH)^-$ was found to be $q=0.8e$, where e is the charge of the electron (in electrostatic units). The effective charge associated with the total area of the 1888.2 and 1901.6 cm^{-1} lines assigned to $(PtH_2)^-$ was found to be $q=2.6e$. Previous experiments on the photopopulation of the other charge states of the PtH and PtH_2 complexes showed that the different charge states have similar IR absorption strengths.[42] Therefore the values of q determined here for $(PtH)^-$ and $(PtH_2)^-$ can also be used for the other charge states of these complexes to estimate their concentrations.

A. Concentrations of Pt-H centers in MIR samples

The areas of the vibrational lines in Fig. 3, spectra (b) and (e), and the calibration of the absorption intensities given above, allow the concentrations of the PtH and PtH_2 complexes in the n- and p-type MIR samples to be estimated. The optical path length for an absorbing layer on the surface of a MIR sample is $x=Lt/(D \sin\theta)$.[31] Here L is the length of the MIR sample, D is its thickness, θ is the bevel angle of the sample's end faces (45° here), and t is the thickness of the absorbing layer. The thicknesses of the surface layers hydrogenated by etching are not well known, so the concentrations of centers per cm^2, Nt, are given for the n- and p-type MIR samples in Table III.

If we estimate a thickness of $t\approx 2.5\ \mu m$ for the hydrogenated layers on each side of the etched MIR samples, based upon typical concentration profiles measured by DLTS for transition-metal H complexes in etched samples [see, for example, Fig. 1(b)], then the concentration of Pt- and H-containing centers is roughly $10^{15}\ cm^{-3}$ in the thin surface layers on each side of the n- and p-type samples. This concentration is in very good agreement with an estimate of the surface hydrogen concentration made previously (also $10^{15}\ cm^{-3}$) from an analysis of the DLTS depth profiles measured for Ag-containing Si that was hydrogenated by etching.[27]

TABLE III. Concentrations of PtH and PtH_2 complexes in the n- and p-type MIR samples whose vibrational spectra are shown in Fig. 3.

Sample	complex	Nt ($10^{11}\ cm^{-2}$)
n type	$(PtH)^-$	3.5
	$(PtH)^0$	1.5
	$(PtH_2)^-$	0.2
p type	$(PtH)^0$	2.0
	$(PtH_2)^0$	0.3

The typical sensitivity limit of vibrational spectroscopy measurements performed at normal incidence is $\approx 10^{17}\ cm^{-3}$ defects for a 1-μm-thick layer (or $10^{13}\ cm^{-2}$).[41] The concentrations of Pt- and H-containing complexes in our MIR samples are roughly two orders of magnitude smaller than this sensitivity limit. The enhanced sensitivity in our experiments results from a combination of the MIR geometry and the narrow widths of the vibrational lines ($\approx$0.4 cm^{-1}) for the PtH and PtH_2 complexes.

B. Concentrations of Pt-H centers in bulk-hydrogenated samples

The calibration of the absorption intensities allows the concentrations of PtH and PtH_2 complexes to be estimated for the bulk-hydrogenated Si samples whose spectra are shown in Fig. 4. The results of an analysis of spectra (a), (b), and (d) from Fig. 4 are shown in Table IV. The total concentrations of PtH and PtH_2 complexes for the different samples are given along with estimates of the total Pt concentration (made from the solubility of Pt in Si) and the fraction of Pt that is hydrogenated. For the sample with a lower Pt concentration, approximately 35% of the Pt is hydrogenated. For the higher Pt concentrations, only $\approx$5% of the Pt is hydroge-

TABLE IV. Concentrations of PtH, PtH_2, and Pt centers in the bulk hydrogenated Si samples whose vibrational spectra [(a), (b), and (d)] are shown in Fig. 4. The fraction of Pt impurities that was hydrogenated is also given.

Sample	[PtH] ($10^{15}\ cm^{-3}$)	[PtH_2] ($10^{15}\ cm^{-3}$)	[Pt] ($10^{17}\ cm^{-3}$)	Fraction
n, [Pt]<[P]	1.2	0.25	0.04	0.35
n, [Pt]>[P]	5.0	0.15	1.0	0.05
p, [Pt]>[B]	3.4	0.15	1.0	0.04

nated. These results confirm that the PtH and PtH_2 complexes are not the dominant defects in the samples and therefore do not determine the position of the Fermi level. For the sample with a lower Pt concentration ($4\times10^{15}\,cm^{-3}$), the P donor is the dominant impurity and the Fermi level lies close to the P donor level at low temperature, as was confirmed here by EPR. For the samples with a higher Pt concentration ($1\times10^{17}\,cm^{-3}$), the estimates in Table IV confirm that isolated Pt is the dominant defect in these samples, consistent with the assumptions made in previous sections.

It is interesting to note that the relatively small concentrations of PtH_2 complexes in our samples give rise to prominent vibrational absorption lines because the value of q for the PtH_2 complex is considerably larger than for PtH, and the strengths of the absorption lines are proportion to q^2. The results in Table IV show that the PtH complex has a concentration roughly 25 times greater than that of PtH_2 in the samples with $[Pt]\approx10^{17}\,cm^{-3}$. (The relatively small concentration of PtH_2 may explain its susceptibility to photoinduced charge state changes in Sec. IV C.)

VI. CONCLUSION

The PtH and PtH_2 complexes in Si have been studied by vibrational spectroscopy and DLTS in the same, or similarly prepared, samples. Samples for IR absorption experiments were also prepared with various positions of the Fermi level by compensation with deep level defects. The Fermi-level dependence of the vibrational spectra has allowed the H-stretching lines of the PtH and PtH_2 complexes to be associated with the specific charge states and electronic levels of these defects that were studied by DLTS. Our experiments show that the DLTS peaks assigned to PtH and PtH_2 complexes in samples hydrogenated by etching at room temperature[16,28] are due to the same defect complexes identified by EPR and vibrational spectroscopies in samples hydrogenated at 1250 °C in an H_2 ambient.[9–11] Furthermore, the correlation of the defect assignments made by structure-sensitive methods[9–11] with the DLTS results[16,28] provides strong support for the method used to assign DLTS peaks to defects with specific numbers of H atoms,[23] i.e., from the depth dependence of the defect-concentration profiles measured for samples hydrogenated by etching. Finally, the combination of DLTS concentration profiles with the vibrational spectra measured for the same samples has led to a calibration of the intensities of the vibrational lines, permitting the concentrations of the PtH and PtH_2 complexes to be estimated from their vibrational spectra.

Vibrational lines that might be associated with defect complexes that contain additional hydrogen atoms, for example, PtH_3 or PtH_4 complexes, have not yet been assigned,[43] even though these defects have been studied by theory[22] and observed by DLTS (Ref. 28) in the near surface region of etched samples where the hydrogen concentration exceeds the Pt concentration. These complexes that contain a greater number of hydrogen atoms are of interest because they might be completely passivated. The identification of their vibrational spectra and the experimental study of their structures remain as a challenge.

ACKNOWLEDGMENTS

We are grateful to G. D. Watkins for numerous helpful discussions and for the use of the EPR spectrometer in his laboratory. We thank M. Kleverman, R. Jones, and A. Resende for discussions of their work prior to publication and for preprints of their papers. We also thank W. B. Fowler, J. P. Huennekens, and S. Knack for their comments on our work. The research performed at Lehigh University was supported by NSF Grant No. DMR-0108914 and NREL Contract No. ACQ-9-29639-02.

*Permanent address: Draper Laboratory, Cambridge, MA 02139.
†Corresponding author. Electronic address: michael.stavola@Lehigh.edu
‡Permanent address: Department of Radiology, MC 2026, University of Chicago, Chicago, IL 60637.
§Permanent address: Infineon Technologies, D-01062 Dresden, Germany.

[1] S. J. Pearton and A. J. Tavendale, Phys. Rev. B **26**, 7105 (1982).
[2] S. J. Pearton and E. E. Haller, J. Appl. Phys. **54**, 3613 (1983).
[3] S. J. Pearton, J. W. Corbett, and M. Stavola, *Hydrogen in Crystalline Semiconductors* (Springer-Verlag, Berlin, 1992).
[4] S. J. Pearton, in *Hydrogen in Semiconductors*, edited by J. I. Pankove and N. M. Johnson (Academic, Boston, 1991), p. 65.
[5] T. Sadoh, H. Nakashima, and T. Tsurushima, J. Appl. Phys. **72**, 520 (1992).
[6] E. Ö. Sveinbjörnsson and O. Engström, Appl. Phys. Lett. **61**, 2323 (1992).
[7] E. Ö. Sveinbjörnsson, G. I. Andersson, and O. Engström, Phys. Rev. B **49**, 7801 (1994).
[8] T. Sadoh, M. Watanabe, H. Nakashima, and T. Tsurushima, J. Appl. Phys. **75**, 3978 (1994).
[9] P. M. Williams, G. D. Watkins, S. Uftring, and M. Stavola, Phys. Rev. Lett. **70**, 3816 (1993).
[10] M. Höhne, U. Juda, Yu. V. Martynov, T. Gregorkiewicz, C. A. J. Ammerlaan, and L. S. Vlasenko, Phys. Rev. B **49**, 13 423 (1994).
[11] S. J. Uftring, M. Stavola, P. M. Williams, and G. D. Watkins, Phys. Rev. B **51**, 9612 (1995).
[12] E. Ö. Sveinbjörnsson and O. Engström, Phys. Rev. B **52**, 4884 (1995).
[13] W. Jost, J. Weber, and H. Lemke, Semicond. Sci. Technol. **11**, 22 (1996); **11**, 525 (1996).
[14] W. Jost and J. Weber, Phys. Rev. B **54**, R11 038 (1996).
[15] J.-U. Sachse, E. Ö. Sveinbjörnsson, W. Jost, J. Weber, and H. Lemke, Appl. Phys. Lett. **70**, 1584 (1997).
[16] J.-U. Sachse, E. Ö. Sveinbjörnsson, W. Jost, J. Weber, and H. Lemke, Phys. Rev. B **55**, 16 176 (1997).
[17] P. Deixler, J. Terry, I. D. Hawkins, J. H. Evans-Freeman, A. R. Peaker, L. Rubaldo, D. K. Maude, J.-C. Portal, L. Dobaczewski, K. Bonde Nielsen, A. Nylandsted Larsen, and A. Mesli, Appl. Phys. Lett. **73**, 3126 (1998).
[18] P. T. Huy and C. A. J. Ammerlaan, in *The Ninth International Conference on Shallow-Level Centers in Semiconductors*, edited by M. Suezawa, H. Nakata, and J. Katayama-Yoshida (Elsevier Science BV, Netherlands, 2001), p. 233 .

[19] M. J. Evans, M. Stavola, M. G. Weinstein, and S. J. Uftring, Mater. Sci. Eng., B **58**, 118 (1999).
[20] R. Jones, S. Öberg, J. Goss, P. R. Briddon, and A. Resende, Phys. Rev. Lett. **75**, 2734 (1995).
[21] A. Resende, R. Jones, S. Öberg, and P. R. Briddon, Phys. Rev. Lett. **82**, 2111 (1999).
[22] R. Jones, B. J. Coomer, J. P. Goss, B. Hourahine, and A. Resende, Solid State Phenom. **71**, 173 (1999).
[23] O. V. Feklisova and N. A. Yarykin, Semicond. Sci. Technol. **12**, 742 (1997).
[24] J.-U. Sachse, E. Ö. Sveinbjörnsson, N. Yarykin, and J. Weber, Mater. Sci. Eng., B **58**, 134 (1999).
[25] M. Shiraishi, J.-U. Sachse, H. Lemke, and J. Weber, Mater. Sci. Eng., B **58**, 130 (1999).
[26] S. Knack, J. Weber, and H. Lemke, Mater. Sci. Eng., B **58**, 141 (1999).
[27] N. Yarykin, J.-U. Sachse, H. Lemke, and J. Weber, Phys. Rev. B **59**, 5551 (1999).
[28] J.-U. Sachse, J. Weber, and E. Ö. Sveinbjörnsson, Phys. Rev. B **60**, 1474 (1999).
[29] J.-U. Sachse, J. Weber, and H. Lemke, Phys. Rev. B **61**, 1924 (2000).
[30] P. M. Mooney, in *Identification of Defects in Semiconductors*, Semiconductors and Semimetals Vol. 51B, edited by M. Stavola (Academic, Boston, 1999), p. 93.
[31] N. J. Harrick, *Internal Reflection Spectroscopy* (Wiley Interscience, New York, 1967).
[32] Following the etching treatment alone, the lines assigned to the two charge states of the PtH complex were seen but with reduced intensity. The heat treatment at 200 °C is believed to liberate additional hydrogen from H_2 molecules that are introduced by the etching treatment that can then interact with Pt.
[33] A speculative assignment is that the 1898.6-cm^{-1} line is due to a Pt- and H-containing complex that also contains an additional transition metal like Cu or Fe, similar to an FeAuH complex that was previously suggested to form in a study of Si containing Au and H (Ref. 19).
[34] *Impurities and Defects in Group IV Elements and III-V Compounds*, edited by O. Madelung and M. Schulz Landolt-Bǒmstein, New Series, Group III, Vol. 22, Pt. b (Springer, Berlin, 1989).
[35] W. Schröter and M. Seibt, in *Properties of Crystalline Si*, edited by R. Hull (INSPEC, London, 1999), pp. 543 and 561.
[36] I. A. Veloarisoa, M. Stavola, D. M. Kozuch, R. E. Peale, and G. D. Watkins, Appl. Phys. Lett. **59**, 2121 (1991).
[37] G. D. Watkins, in *Handbook of Semiconductor Technology*, edited by K. A. Jackson and W. Schröter (Wiley-VCH, Weinheim, 2000) Vol. 1, Chap. 3.
[38] In a few samples, IR lines due to hydrogenated lattice defects [B. Bech Nielsen, L. Hoffman, M. Budde, R. Jones, J. Goss, and S. Öberg, Mater. Sci. Forum **196–201**, 993 (1995)] were also produced by the electron irradiation. These were not the dominant defects in the samples as was confirmed by our IR and EPR measurements of the charge states of the A center and E center that were used to confirm the location of the Fermi level in the samples.
[39] R. C. Newman, *Infrared Studies of Crystal Defects* (Taylor and Francis, London, 1973).
[40] The peak absorbances of only the antisymmetric-stretching lines were measured for the different charge states of the PtH_2 complex to determine the fraction of defects in each charge state.
[41] M. Stavola, in *Identification of Defects in Semiconductors* (Ref. 30), p. 153.
[42] In Ref. 11, it was found that filtering the spectrometer light caused changes of the populations of the different charge states of the PtH and PtH_2 complexes and therefore changes in the intensities of the vibrational lines assigned to different charge states. The changes in the areas for the different charge states of the same defect were approximately equal in magnitude and opposite in sign, showing that the different charge states have approximately the same value of q.
[43] There are several vibrational lines that were observed in Si that contains Pt and H that might possibly be due to complexes of Pt with more than two H atoms (Ref. 11). These lines were seen only in samples that had been quenched very quickly following the H-introduction anneal at 1250 °C. Because these vibrational lines have been seen only infrequently in our studies, it has not yet been possible to assign them to specific defect complexes.